Hittite Journal of Science and Engineering, 2017, 4 (1) 31-37
ISSN NUMBER: 2149-2123
DOI: 10.17350/HJSE19030000045

Design and Analysis of In-Drum Outer Rotor BLDC Motor for Eddy Current Separator

Ahmet Fenercioglu[1] and Merve Sen Kurt[2]
[1]Gaziosmanpasa University, Department of Mechatronic Engineering, Tokat, TURKEY
[2]Amasya University, Department of Electric and Electronics Engineering, Amasya, TURKEY

ABSTRACT

In this study, a novel In-Drum Brushless Direct Current (ID-BLDC) motor is proposed to Eddy Current Separator (ECS) which separates nonferrous metals from waste. The ECS's separation efficiency depends on magnetic drum speed. ID-BLDC motor is designed with outer rotor structure and placed in ECS magnetic drum in order to improve separation efficiency. The magnetic drum is directly driven by this motor because it doesn't require coupling mechanisms. It has very simple structure since no rotor windings, brushes and bracelets. The ID-BLDC motor has high reliability, high efficiency and high power-to-volume ratio. Proposed motor has 8 poles, 3 phases, 373 W (0.5 HP) and 1750 rpm rated speed. Output parameters are calculated for full load and verified by Finite Element Analysis (FEA) under the over load, full load, half load, quarter load and no load conditions for transient and steady state.

Article History:
Received: 2017/02/02
Accepted: 2017/04/05
Online: 2017/06/30

***Correspondence to**: Merve Sen Kurt, Amasya University, Department of Electric and Electronics Engineerin, Amasya, TURKEY.*
Tel: +90 (358) 260-0066 (1468)
E-Mail: mervesenkurt@gmail.com

Keywords:
Brushless motors; Outer rotor motors; Permanent magnet motors; Finite element analysis (FEA); Eddy current separator

INTRODUCTION

ECS is a machine that provides recycling via separation of nonferrous metals by means of the eddy current effect. It separates copper, aluminum, brass, silver and similar valuable metals from wastes. The most important component of ECS that affects separation performance is magnetic drum. Higher rates of rotation and the multipolarity of the magnetic drum results in greater magnitudes of eddy currents in the metal that will be separated according to Faraday principles. In this case, the separation efficiency increases, while making the separation of smaller sized particles possible [1].

In General ECS, the drum is driven by a coupled motor. This motor rotates the drum directly by coupling or with a belt and pulley mechanism. In this case, reaching higher speeds is difficult due to loss in transfer organs and the balance effect. ECS machine and working principle scheme are given in Fig.1.

This study proposes the design of an outer rotor BLDC motor to be installed in the drum to increase the ECS performance and to separate metals with small particle sizes. A BLDC motor consists of a stator with coils, a rotor with permanent magnets, position sensors and driver circuits. The driver circuits assume the role of the brush collector setup of classic brushed DC motors, while the position sensors provide the rotor position data to the controller. Based on position data and the rotation direction, the controller excites the related motor phase.

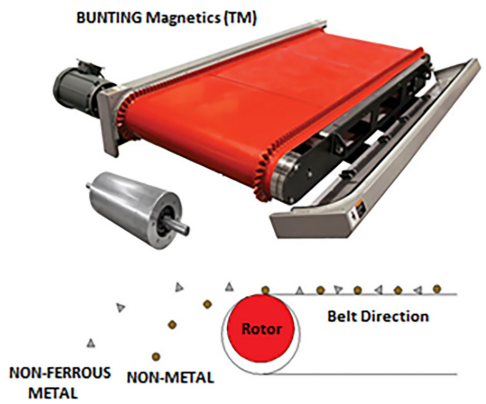

Figure 1. ECS machine and working principle (BUNTING Magnetics (TM)).

BLDC is placed in a drum with an out runner rotor. In these types of motors, the stator is fixed at the center of the motor and the rotor made of permanent magnets rotates around the stator. It drives the drum directly without a requirement of motion transfer organs. Hence, it has a higher efficiency due to the fact that there is no mechanical transfer loss and that it can work at high rates. The motor requires less space since it is located in the drum in comparison with drums that are driven externally and it is also aesthetically pleasing.

Literature surveys carried out put forth that there are no studies related to the application of BLDC motor in the drum. However, there are several studies about outer rotor BLDC designs. Some of these studies are summarized below:

In outer rotor BLDC motors, the width of the stator slots significantly affect the produced cogging torque. It was observed that BLDC motors designed with wide slots produced higher cogging torque [2].

The geometric structure and basic parameters (PM angle, PM residual induction, PM relative permeability, PM height, rotor yoke height) of permanent magnets that are present in the outer rotor BLDC motors affect the magnetic flux generated in the air gap. The change in magnetic flux generated for various parameters was analyzed by finite elements method by taking the geometric structure of the permanent magnets and the nonlinear characteristics into account [3].

The armature flux generated by the current passing through the BLDC motor's stator coils is omitted when the motor runs in an unsaturated area. However, when the motor is run in a saturated area, it is stated that this effect grows, disrupts the air gap flux density thus failing to reach a uniform torque distribution [4].

The outer rotor BLDC motor drives with permanent magnets were also covered for electrical and hybrid vehicles. The machine topology, driver operations and control strategies were emphasized [5].

An outer rotor BLDC motor was designed for light traction at low rates using finite elements method (FEM). Rate, phase current, power and torque curves with respect to time were assessed to observe the performance of the designed motor's [6].

A hybrid permanent magnet hydrodynamic bearing was designed. It works passively and contactless. Various permanent magnet topologies are studied and analyzed by FEM in terms of axial forces and stiffness [7].

It was studied about a current distribution control on dual direct-driven wheel motors for electric vehicles. The vehicle dynamics and control strategy are modeled and the control performance is simulated numerically [8].

The application of the VSS (variable structure system) approach to the position control of an AC brushless servo motor is discussed. A DSP (digital signal processor) is used to make the time needed to calculate the control input [9].

H2 and H∞ controllers were designed for a permanent-magnet synchronous motor drive system without using shaft position sensor, and presents the field-weakening control algorithm of the drive system. [10].

In this study, a BLCD motor design was proposed for an ECS magnetic drum drive. The motor has an outer rotor and is placed in the drum. This way, the system has a high efficiency, as is the case for direct drive, since there will be no power transfer losses in the drum. This predicted motor design was verified for the predicted system via analytical methods and magnetic analyses were carried out for various loads via finite elements methods. In these analyses, torque, phase currents and rate parameters were calculated for temporary and permanent states, and presented with graphs.

ID_BLDC MOTOR

The ID-BLDC motor is an outer brushless DC motor that is placed in the drum. The stator of this motor is fixed and attached to a fixed shaft. The rotor is coupled to the drum and provides motion. Permanent magnet poles are used in the motor's rotor. The power/volume ratio of the motor is high due to the additional power provided by the magnets. As such, the proposed motor can easily be placed in the drum due to its smaller size. Since the motor has an outer rotor, it provides advantages such as high torque and less noise [11], due to the increased rotor diameter. The only disadvantage of ID-BLDC motors is difficulty in cooling since it is inside the stator. However, since the motor in ECS works under the constant load, the motor works at nominal current. Therefore, overheating does not occur.

Motor Selection

The weight of the drum (m), inertia moment (J), angular acceleration (α) and motor speed (n) were taken into account in order to determine the predicted motor power. The drum in which the ID-BLDC was placed in is shown in Figure 2a and Figure 2b. The length of the drum ld = 0.3 m, the outer radius R1 = 0.056 m and the inner radius is R2 = 0.046 m.

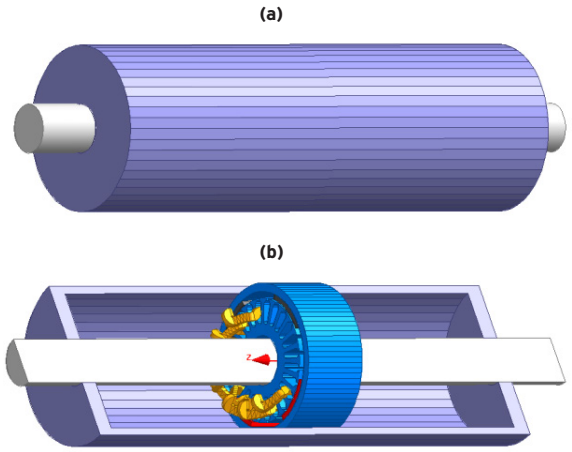

Figure 2. a) Drum, b) ID-BLDC motor inside of the drum

The acceleration time it took for the motor to reach the rated speed was taken as 3 seconds. With these data at hand, the volume and specific weight of the drum were initially considered, and the mass (m) of the drum was calculated as approximately 10 kg. To determine the inertial moment, the gyration radius (R0) is calculated using Equation 1:

$$R_0 = \sqrt{\frac{R_1^2 + R_2^2}{2}} \tag{1}$$

From this point, the inertial moment is calculated with Equation 2:

$$J = mR_0^2 \tag{2}$$

The torque required to bring the drum to its rated speed in 3 seconds is calculated with Equation 3:

$$T = j\alpha \tag{3}$$

Using these equations, the moment is calculated as 1.59 Nm. When the 1750 rpm rate is taken into account, the required motor power is found as 291.38 W by using Equation 4. The nominal power of the motor is proposed as 0.5 HP (373 W) by taking the losses into consideration.

$$P = T\omega \tag{4}$$

The ID-BLDC motor can be controlled with an appropriate BLDC motor driver. Table 1 consists of nominal values of the ID-BLDC motor.

The ID-BLDC motor can be controlled with an appropriate BLDC motor driver. Table 1 consists of nominal values of the ID-BLDC motor.

Table 1. Rated values of the IN-BLDC motor

Nominal elements of the formulas	*Nominal Value*
Output Power (HP)	*0.5*
Voltage (V)	*220*
Current (A)	*1.76*
Efficiency (%)	*82.92*
Speed (rpm)	*1750*
Torque (Nm)	*1.75*

Table 2 shows the model's dimensions, and Figure 3 shows the cross-sectional view of the model.

Table 2. ID-BLDC motor dimensions

Symbol	*Quantity*	*Size*
D_{RI}	*Rotor Inner Diameter*	*0.082 m*
D_{RO}	*Rotor Outer Diameter*	*0.092 m*
D_{SH}	*Shaft Diameter*	*0.03 m*
D_{SI}	*Stator Inner Diameter*	*0.03 m*
D_{SO}	*Stator Outer Diameter*	*0.074 m*
L_{SL}	*Stack Length*	*0.04 m*
L_G	*Air Gap Thickness*	*0.001 m*
N_R	*Number of Rotor Poles*	*8*
N_S	*Number of Stator Poles*	*24*
θ_M	*Magnet Degree*	*0.79 rad*

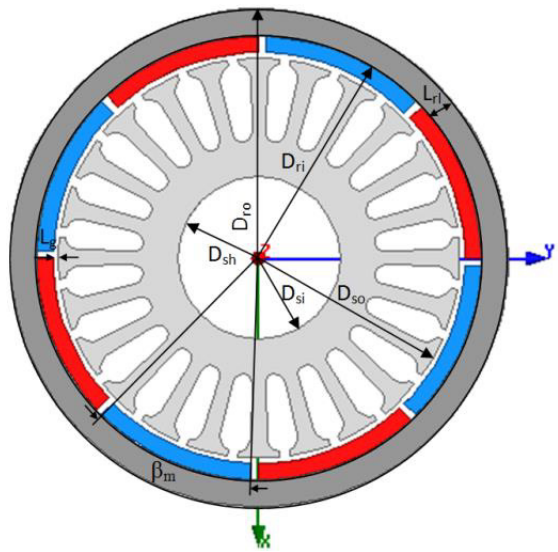

Figure 3. ID-BLDC's cross section and dimension expressions

Electromagnetic Model of ID-BLDC

Core reluctance was omitted as the air gap and the magnetic reluctance are high in BLDC motors, In this case, the air gap reluctance (R_g) and the permanent magnet reluctance (R_m) in the magnetic circuit of an ID-BLDC, as seen in Figure 4, is calculated using Equation 5. Where l_g is air gap distance and l_m is magnet length, S is the effective surface area of stator pole.

$$R_g = \frac{l_g}{\mu_0 s} \qquad R_m = \frac{l_m}{\mu_m s} \tag{5}$$

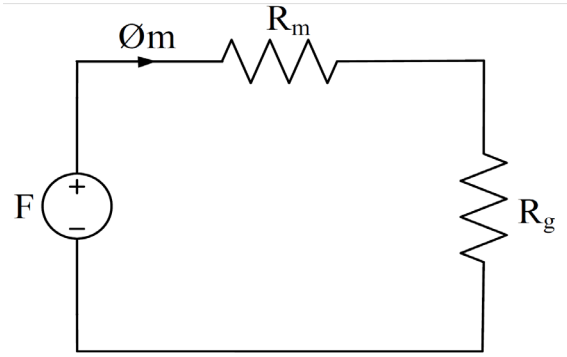

Figure 4. a) Drum, b) ID-BLDC motor inside of the drum

If magnet permeability (μ_m) and vacuum permeability (μ_0) are assumed to be equal ($\mu_m=\mu_0$) the total reluctance of the magnetic circuit is expressed as shown in Equation 6 [12].

$$R_t = R_g + R_m = \frac{l_g + l_m}{\mu_0 s} \tag{6}$$

Magnetic permanence (ρ_o) is calculated via Equation 7:

$$\rho_0 = \frac{1}{R_t} = \frac{\mu_0 s}{l_g + l_m} \tag{7}$$

The total flux (ϕ) in magnetic circuit shown in Figure 4 [13]. Where B_m, B_g are magnet and air gap magnetic flux densities, A_m, A_g are the cross sectional areas of magnet and air gap respectively. H_g is the magnetic field intensity in air gap.

$$\phi = B_m A_m = B_g A_g = \mu_0 H_g A_g \tag{8}$$

The magnetic flux density (B_m) is found by using Equation 9 [13]. Where μ_r is the relative permeability and H_m is the magnetic field intensity in the magnet.

$$B_m = \mu_r \mu_0 H_m \tag{9}$$

Equation 10 is derived from Equation 8 and Equation 9:

$$\phi = \mu_r \mu_0 H_m A_m \tag{10}$$

Magneto motive force (F) is found by using Equation 11:

$$F = \phi R_t = NI = l_m H_m + l_g H_g \tag{11}$$

Where N is the number of turn. The current (I) passing through the stator coils is derived from Eq.11 and is calculated by Eq.12 [14].

$$I = \frac{\phi R}{N} \tag{12}$$

The power (P) is supplied from the network is found by using Equation 13. The rated voltage applied on the motor is 220 V DC.

$$P = UI \tag{13}$$

Basically torque can be calculated by using Equation (4). The efficiency is output mechanical power (Pm) to input electrical power (Pi) ratio. Electrical and mechanical powers are found Eq.13 and Eq. 4 respectively.

ASSUMPTIONS

The magnetic flux in the core is assumed to be uniform in analytical calculations. The saturation effects were not taken into account and BH characteristic of the core material was assumed to be linear.

The analyses were carried out using ANSYS/Maxwell program which solves equations via 2D finite elements method. M19 material was used as core material. The BH curve of this material is given in Figure 5. The NdFeB (N35) magnets are allocated on rotor surface. For the motor control, a standard BLDC motor drive was used. In FEA, motor is driven by external circuit. This circuit is taken into consideration, voltages and speed are accepted as constant in steady state.

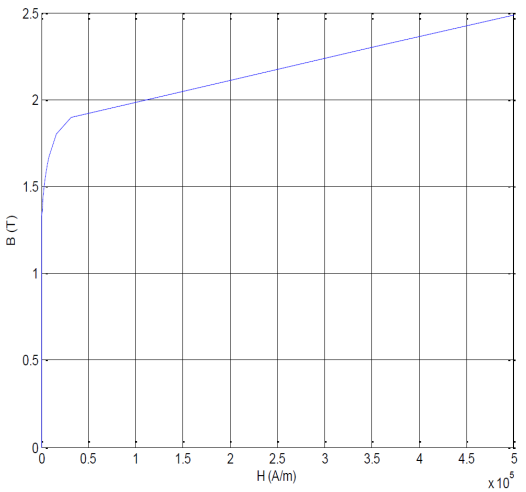

Figure 5. BH curve of M19 material

FINITE ELEMENT ANALYSIS (FEA)

2D transient analyses of proposed motor were carried out with FEA software AnSys Maxwell. For the analysis, the calculations were obtained for no-load, 25%, 50%, full-load, 125%, and overload (150%) conditions. The change in speed with respect to time are shown in Figure 6, with taking the FEA transient results into account. Figure 6a shows the change in speed with respect to load in transi-

ent state, and Figure 6b shows the average change in speed for steady-state conditions.

As can be seen in Figure 6a, the motor reaches steady state after 60 ms. And as seen in Figure 6a and 6b, as the motor load increases, the decrease in armature voltage and the flux in air gap increases, causing the decrease in motor speed.

For various loads of the ID-BLDC motor, Figure 7a shows the transient torque change, and Figure 7b shows the average electromagnetic torque curves for steady state.

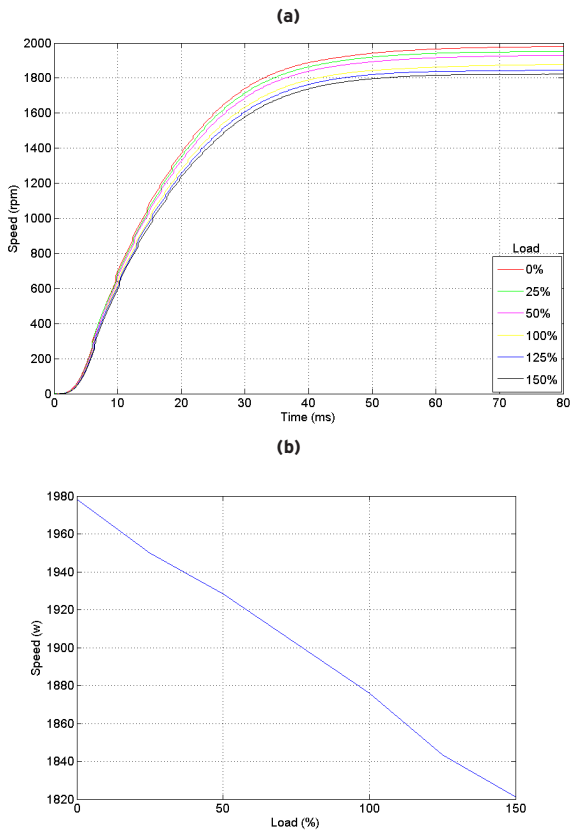

Figure 6. ID-BLDC change in motor rate a) transient rate b) steady state average rate

From Figure 7b, it can be seen that the torque increases with increasing load. With increasing current, the flux in the core increases. According to the BH characteristics, saturation in the core begins approximately at 1.5 T. In the saturated zone, the increase magnetic flux in the saturated zone does not increase proportionally with current; therefore the torque does not increase in the similar proportion. It is seen that after full-load, the average torque value increases less when compared to increasing load. The phase currents diagrams are shown in Figure 8. The phase current for full-load is calculated as 1.88 A in rms. The phase approximately has a sinusoidal profile. It is seen that in the starting, motor phase currents are too much, and it reaches its rated value after 60 ms.

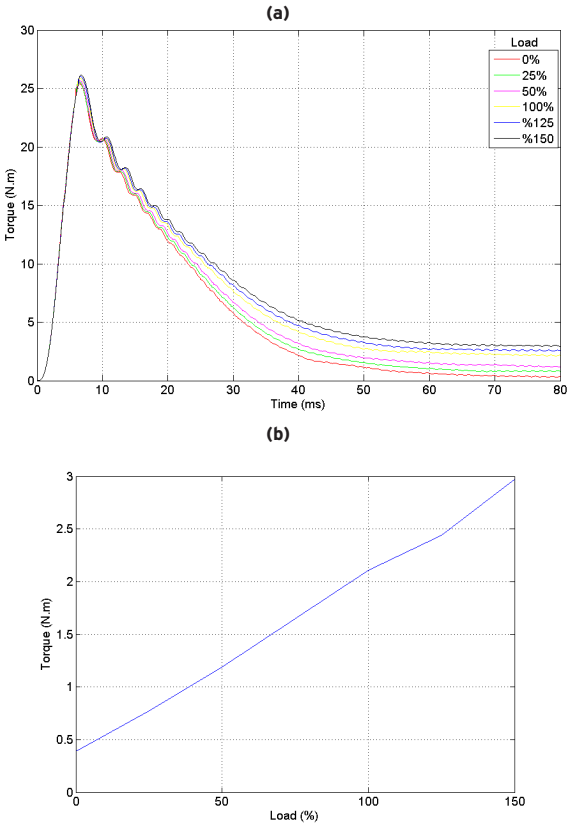

Figure 7. ID-BLDC motor electromagnetic torque profile a) transient torque b) steady state average torque

The stator magnetic flux density distribution of ID-BLDC motor at full-load is given in Figure 9. Flux density distributions have been shown a) vector at Figure 9a, b) magnitude at Figure 9b and c) flux curves at Figure 9c.

The BH curves of the core material chosen in the analyses are shown in Figure 5. The saturation begins after 1.5 T in this material. Saturation begins at stator slot teeth in flux

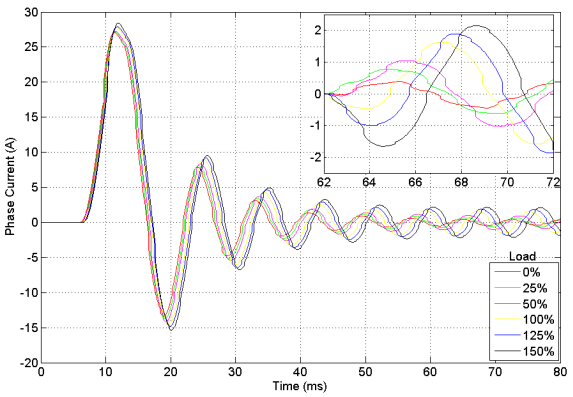

Figure 8. Phase currents according to load

distributions. There is approximately 1.2 T magnetic flux density in the rotor and the air gap. Additionally, the air gap flux density was calculated as 1.23 T analytically from the magnetic model. FEA and analytical results are compared in Table 3.

CONCLUSION

ECS are commonly used to separate and recycle nonferrous valuable metals such as copper, aluminium from waste. The most important component that affects ECS separation efficiency is the magnetic drum. The drum must be rotated at high speeds in order to separate small metals in form of granules. The losses are great and speed limits occur when the drum is driven via coupling, sprockets or belt-pulleys.

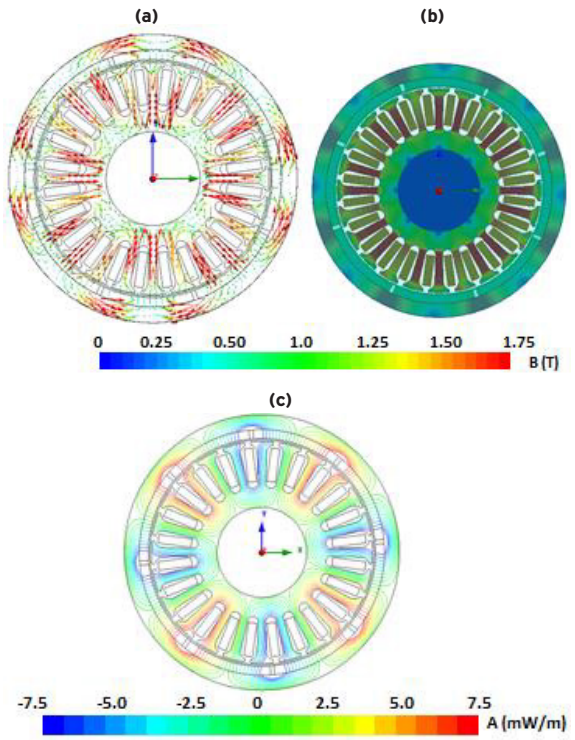

Figure 9. Flux distributions a) vector b) magnitude c) flux lines

Table 3. FEA and analytical results of motor output values at full-load

Results	Current(A)	Torque (Nm)	Power (W)	Rate (rpm)
FEA	*1.88*	*2.106*	*414*	*1750*
Analytical	*1.64*	*1.98*	*361.7*	*1750*

In this study, the BLDC motor has designed with outer (external) rotor and it has placed in the drum and driven directly. It has called ID-BLDC motor. The magnetic drum can reach high speeds with this motor thus making it possible to separate and recover small particles. In addition, the motor will cover less space while being aesthetically appealing since it will be completely in the drum.

The proposed motor has no brushes, bracelets, salient poles and rotor winding. Proposed new ECS drum which driven by ID-BLDC motor has no power transfer mechanisms. Thus it decreases the losses and the required maintenance, and has the motor works quietly. It can be reach high speed.

The motor power selected 0.5 HP (373 W) according to the drum dimensions. Designed ID-BLDC motor's rated values are 220 V, 1.71A, 1750 rpm, 1.70 Nm, %83 efficiency. Electrical and magnetic parameters such as power requirement of drum, magnetic reluctance, flux density, magneto motive force, current, torque, speed, efficiency and power were examined. Parameters were predicted by analytical calculations and verified by FE analyses for different load conditions. In full load, the power is calculated 371,7 W in analytical predictions and analyzed 414 W in FEA. Analytical solutions were made in linearity. FEA solutions were taken into consideration non-linearity and BH curve of the material. Thus the difference is in acceptable limits.

This ID-BLDC motor is an original study. It is proposed for a new ECS drum design to improve separation efficiency.

REFERENCES

1. Rem PC, Beunder EM, van den Akker AJ. Simulation of eddy–current separators. IEEE Transactions on Magnetics 34 (1998) pp. 2280–2286.
2. Nizam M, Waloyo HT, and Inayati. Design of optimal outer rotor brushless dc motor for minimum cogging torque, 2013 Joint Int. Conf. on Rural Inf. & Communication Technol. and Electr.–Vehicle Technol. (rICT & ICeV–T), Bandung–Bali, İndonesia, 2013, pp. 1-4.
3. Dirba J, Lavrinovicha L, Onzevs O, Vitolina S. The influence of permanent magnet parameters on the effectiveness of brushless DC motor with outer rotor, 2012 Int. Conf. on Power Electronics Electr. Drives, Automation and Motion (SPEEDAM), Sorrento, Italy, 2012, pp. 718–723.
4. Kerdsup B, Fuengwarodsakul NH. Analysis of brushless DC motor in operation with magnetic saturation using FE method, 2011 8th Int. Conf. on Electr. Eng. Electronics, Comput. Telecommun. And Inf. Technol. (ECTI–CON), Khon Kaen, Thailand, 2011, pp. 629-632.
5. Chau KT, Chan CC, Chunhua L. Overview of permanent–magnet brushless drives for electric and hybrid electric vehicle. IEEE Transactions on Industrial Electronics 55 (2008) pp. 2246–2257.
6. Lopez–Fernandez XM, Gyselinck J. Design of an outer–rotor permanent–magnet brushless DC motor for light traction through transient finite element analysis, 2016 Int. Conf. on Computational Electromagnetics (CEM), Aachen, Germany, 2006, pp. 1–2.
7. Pohlmann A, Hameyer K. A study permanent magnet topologies for hybrid bearings for medical drives applied in ventricular assist devices. Archieves of Electrical Engineering 60 (2011) pp. 371–380.
8. Yang YP, Lo CP. Current distribution control of dual

directly driven wheel motors for electric vehicles. Control Engineering Practice 16 (2008) pp. 1285–1292.
9. Hashimoto H, Nakayama T, Kondo S, Harashima F. Practical variable structure approach for brushless servo motor control practical implementation of DSP, 19th Annu. IEEE Conf. on Power Electronics and Specialists, Kyoto, Japan, 1988, pp. 207–213.
10. Liu TH, Cheng CP. Controller design for a sensorless permanent–magnet synchronous drive system. IEE Proc. B–Electr. Power Applications 140 (1993) pp. 369–378.
11. Lelkes A, Krotsch J, Doncker RW. Low–noise external rotor BLDC motor for fan applications, 37th IAS Annu. Meeting on Ind. Applications Conf., USA, 2002, pp. 2036–2042.
12. Wu H, Wang Z, Lv X. Design and simulation of axial flow maglev blood pump. I. J. Inf. Engineering and Electronic Business 2 (2011) pp. 42–48.
13. Fitzgerald AE, Kingsley C, Umans SD. Electric Machinery, sixth ed. McGraw–Hill, New York, 2002.
14. Hemati N, Leu MC. A complete model characterization of brushless DC motors. IEEE Transactions on Industrial Applications 28 (1992) pp. 172–180.